AIP ADVANCES **8**, 055135 (2018)

Unconventional large linear magnetoresistance in $Cu_{2-x}Te$

Ali A. Sirusi,[1] Alexander Page,[2] Lucia Steinke,[1] Meigan C. Aronson,[1] Ctirad Uher,[2] and Joseph H. Ross, Jr.[1,a]
[1]*Department of Physics and Astronomy, Texas A&M University, College Station, Texas 77843, USA*
[2]*Department of Physics, University of Michigan, Ann Arbor, MI 48109, USA*

(Received 12 May 2017; accepted 21 May 2018; published online 31 May 2018)

We report a large linear magnetoresistance in $Cu_{2-x}Te$, reaching $\Delta\rho/\rho(0) = 250\%$ at 2 K in a 9 T field, for samples with $x = 0.13$ to 0.22. These results are comparable to those for Ag_2X materials, though for $Cu_{2-x}Te$ the carrier densities are considerably larger. Examining the magnitudes and the crossover from quadratic to high-field linear behavior, we show that models based on classical transport behavior best explain the observed results. The effects are traced to the misdirection of currents in high mobility transport channels, likely due to behavior at grain boundaries such as topological surface states or a high mobility interface phase. The resistivity also exhibits a T^2 dependence in the temperature range where the large linear MR appears, an indicator of electron-electron interaction effects within the high mobility states. Thus this is an example of a system in which electron-electron interactions dominate the low-temperature linear magnetoresistance.
https://doi.org/10.1063/1.4994071

I. INTRODUCTION

Considerable attention has been devoted to systems exhibiting linear magnetoresistance (MR), starting with effects observed in Ag_2Te and Ag_2Se.[1,2] In these systems linear MR extends to very large applied fields, in contrast to conventional conductors exhibiting quadratic MR which eventually saturates with increasing field. The origin of the effect in Ag_2Te and Ag_2Se is likely associated with topological surface states,[3–6] although other mechanisms have been proposed.[7] Meanwhile many related systems have been discovered to exhibit a large linear MR, including Dirac semimetals,[8–10] and there is considerable interest in the classical and quantum mechanisms that can underlie these phenomena.

Models proposed to explain the Ag_2X effects include the quantum mechanism of Abrikosov,[11] with orbital quantization in relatively small fields attributed to low-mass carriers due to disorder-induced band contact. Weak anti-localization[12,13] can also be important for surface state magnetotransport, and the interplay of these effects with linear MR has been examined, for example, in Bi_2Te_3-based topological insulators.[14,15] On the other hand Parish and Littlewood[16,17] showed that a classical mechanism gives linear MR over a wide range of fields in the case of a distribution of carrier mobilities significantly exceeding the mean value ($\Delta\mu \gg \langle\mu\rangle$). Herring[18] earlier showed that linear MR can occur in weakly inhomogeneous systems if the cyclotron orbit period exceeds the scattering time, equivalent to $B\langle\mu\rangle > 1$. A common feature of these models is low mass/high mobility states required to initiate linear MR in small fields.

With linear MR in Ag_2Se observed to track with mobility,[19] a classical model appears to apply. Nevertheless the origin remains unclear since small fields are also needed to limit carriers to the

[a]jhross@tamu.edu

lowest Landau level within the topological surface states of these systems,[3] suggesting a quantum mechanism. It was further proposed[7] that more conventional processes involving compensating charge carriers may dominate in Ag_2Te, and a mechanism based on spin splitting of surface states has also been advanced for topological insulators.[20] Weak antilocalization as a bulk rather than surface effect[13] may also occur in these layered systems in the presence of spin-orbit coupling. Furthermore it was recently demonstrated[10] that even very weak disorder may lead to such effects in 3D high-mobility systems such as the Dirac semimetals.

Cu_2Te has been of significant interest for potential applications including thermoelectric and solar energy conversion, as well as a variety of nano-devices,[21–24] and it has been connected to a topologically nontrivial band configuration.[25,26] Synthesized bulk materials have stoichiometry $Cu_{2-x}Te$, with the Cu deficit forming vacancies which lead to *p*-type carriers. Here we present magnetotransport results for materials in the range x = 0.13 to 0.22. The large linear MR is traced to high mobility threading carriers in a classical model, and occurs in a regime of high carrier density and with strong electron interactions distinct from what has been observed in other systems.

II. EXPERIMENTAL METHODS

The three polycrystalline samples were obtained by solid state reaction and vacuum annealing. Their properties are described in more detail in Ref. 27. Compositions from electron microprobe measurements are $Cu_{1.87}Te$, $Cu_{1.82}Te$, and $Cu_{1.78}Te$ (x = 0.13 to 0.22), with Hall measurements showing them to be heavily-doped *p*-type semiconductors with room temperature carrier densities 3.6, 4.1, and 6.5×10^{21} cm^{-3}, respectively. The results along with NMR measurements are consistent with a Fermi level in the bulk which is pulled below the valence band edge due to Cu deficit,[27] with room temperature Hall results matching the expected bulk carrier densities. The structure for $Cu_{1.87}Te$ and $Cu_{1.82}Te$ is a superstructure of the hexagonal Nowotny structure,[27,28] with a somewhat different superstructure for the $Cu_{1.78}Te$ case. Measurements reported here utilized a Quantum Design PPMS system and a Quantum Design MPMS combined with an AC bridge. Transport measurements were performed on bar-shaped samples cut from the polycrystalline ingots, with magnetoresistance measured in the geometry with the field perpendicular to the current.

III. RESULTS AND ANALYSIS

Figure 1 exhibits resistivities below 60 K. The behavior is quadratic in the low-temperature limit, particularly for the lowest-vacancy composition: fitting to $\rho_0 + AT^n$ below 30 K yielded n = 2.02, 2.13 and 2.34 for increasing x. Extended to room temperature, the residual resistivity ratios are 32, 31, and 14 for the samples with increasing x. The inset of Fig. 1 also shows carrier densities derived from the

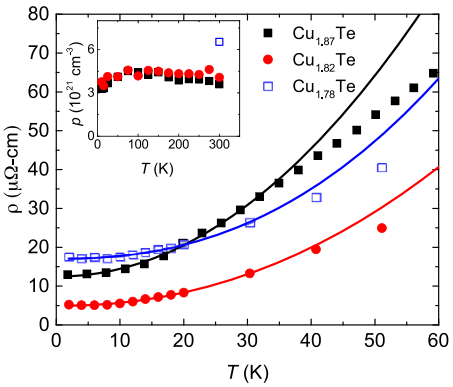

FIG. 1. Resistivity vs. T for three $Cu_{2-x}Te$ samples at low temperatures. Solid curves are T^n fits as explained in text. Inset: Hall effect-derived carrier densities.

Hall resistances, shown vs. temperature for $Cu_{1.87}Te$ and $Cu_{1.82}Te$. These show a low temperature downturn where the T^2 resistivity sets in, likely a result of changing conduction paths rather than a reduction in the bulk carrier density.

Fixing the low-temperature exponent to $n = 2$, the fitted resistivity pre-factors are $A = 0.019$, 0.009, and 0.010 $\mu\Omega$cm/K^2 for the three samples with increasing x. These compare to the lower end of the range for Fermi liquid behavior in heavy-Fermion materials,[29] although with the low-temperature behavior due to high-mobility transport channels, this implies considerably smaller effective A values within these channels, comparable for example to elemental transition metals. Mobilities derived from the resistivities and room-temperature carrier densities are $\mu = 10$ cm^2/Vs or less at room temperature, increasing to 170, 280, and 55 cm^2/Vs for $Cu_{1.87}Te$, $Cu_{1.82}Te$, and $Cu_{1.78}Te$ respectively at 2 K. These are not unexpected for semiconductors with large vacancy densities and

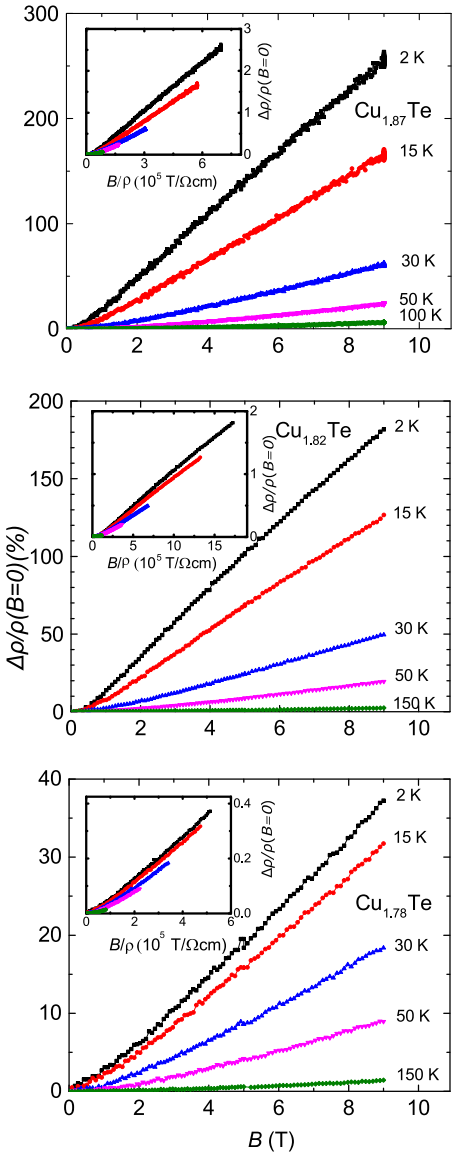

FIG. 2. Magnetoresistance as a function of magnetic field for the three samples at temperatures 2 K, 15 K, 30 K, 50 K, and 100 K or 150 K as shown. The insets are Kohler plots.

large hole band mass[25] close to 0.5 m_e, although the temperature dependences are large for such a case.

Figure 2 displays the magnetoresistance, MR = $\Delta\rho/\rho(0)$, where $\Delta\rho = [\rho(B) - \rho(0)]$, and $\rho(B)$ denotes the resistivity measured in applied field B. The 2 K magnitudes reach 250%, 180%, and 37% at 9 T for $Cu_{1.87}Te$, $Cu_{1.82}Te$, and $Cu_{1.78}Te$, respectively. The largest of these are comparable to effects observed[1] in Ag_2Te, although differing in that the Ag_2Te results are observed in a much narrower composition window for carrier densities near zero, and decrease more slowly vs. temperature.

The insets of Fig. 2 also display Kohler plots, often used to understand whether a single scattering process controls the magnetoresistance.[30] The curves deviate from a common line at 30 K and below, showing that there are different scattering processes corresponding to the low-temperature conduction mechanism.

Fig. 3(a) shows crossover fields (B_c), where the MR changes from quadratic to linear. B_c was obtained by fitting the low-field resistivity to a B^2 dependence, and linear at higher fields, and

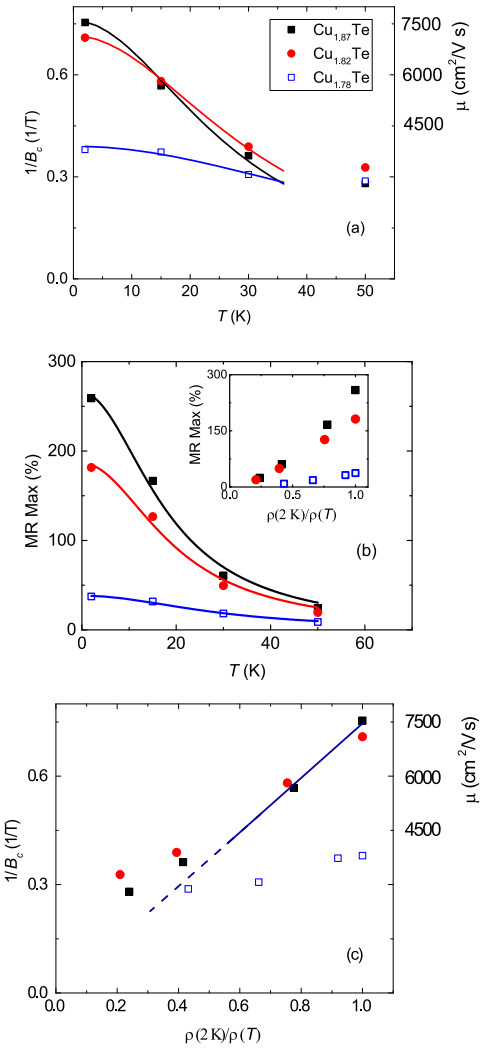

FIG. 3. (a) Crossover field vs. T for the three samples, with average mobility corresponding to the Parish-Littlewood crossover condition on the right axis. (b) 9 T MR values vs. T, and (inset) vs. scaled inverse resistivity. Trendlines in plots (a) and (b): $1/(a + bT^2)$ curves. (c) Crossover field vs. normalized inverse resistivity, with straight line through origin as guide to the eye. Symbols are common to all plots.

extracting the fields where these curves cross.[9] The very small response for the highest measured temperatures could not be fitted.

In the Parish and Littlewood (PL) model, B_c is related to the average mobility through $B\langle\mu\rangle = 1$. For discontinuous classical transport cases, based on numerical simulations[31] it appears that a similar condition, $B_c\mu \simeq 1$, characterizes the crossover field, where μ is the mobility of percolating high-mobility carriers rather than a mean value. In Fig. 3(a) average mobility values are given on the right axis according to the PL condition. For the two lowest-x samples these are close to 7500 cm^2/Vs at 2 K, considerably larger than the Hall mobilities extracted for these samples. Thus in the case that classical transport drives the linear MR, there must be high mobility regions within the overall low mobility material, or a more continuous broad distribution with a range encompassing such characteristic higher mobility values. Clearly the case of relatively weak disorder[18] cannot account for the behavior, since the crossover fields are well out of range of the nearly-uniform high mobility needed for this to work.

For carriers of one sign, in the PL model the magnitude of the linear MR also scales with average mobility, and in some cases a direct proportionality has been observed. As a measure of the linear MR we plotted the 9 T values (MR Max) vs. T in Fig. 3(b). In the inset these are plotted vs. the normalized inverse resistivities measured at the corresponding temperatures, a measure of the mobilities for the case of constant carrier densities as we have here. However the plots are not linear, reflective perhaps of a discontinuous mobility distribution rather than the distributed inhomogeneity of the PL model.

A more direct connection to the mobility is provided by the plot of $1/B_c$ vs. inverse resistivity normalized to 2K, Fig. 3(c). In this case the two lowest-x samples fall very close to the same line through the origin below 30 K. These samples exhibit the largest MR, and resistivities closest to T^2 within the same temperature regime below 30 K. Normalized in this way, the changes in resistivity will be proportional to changes in mobility if a single carrier type dominates. This would be consistent with a discontinuous classical transport mechanism if high mobility threading carriers begin to dominate the measured resistivities below 30 K. The $1/(a + bT^2)$ curves in Fig. 3(a) and (b) are also drawn to correspond to this relation, showing that MR Max also connects approximately to the inverse of the mobility at low temperatures.

A plot of $1/B_c$ vs. MR max is also given in Fig. 4, and we see that there is a universal scaling between these quantities for all samples. A straight-line relationship is expected for a classical transport model, but with zero intercept in the PL model. This result is also similar to the universal scaling identified in Ref. 32 for nanoparticle films, although again in the present case there is a large offset. Note however that other systems have been observed to exhibit such an offset, for example in results for Ag_2Se films[19] one can see that the corresponding offset has a much larger value of about –23 T^{-1}. The reasons for this behavior are not entirely clear.

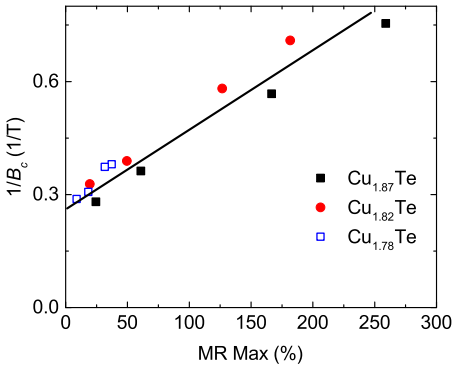

FIG. 4. Inverse crossover field plotted vs. maximum MR (9 T values) for the $Cu_{2-x}Te$ samples at 2 K. Straight line is guide to the eye.

Aside from a threading state mechanism, because of its layered nature 2D weak anti-localization of spin-orbit-split states in the bulk could play a role in Cu_2Te. Such effects can be difficult to separate from classical linear MR, and the corresponding magnetoconductance[12] indeed works reasonably well as an alternative fitting model for the present data (not shown). These fits, with addition of a large quadratic classical magnetoconductance term, yield maximum dephasing lengths[12] at 2 K between 19 and 30 nm, not unreasonable values. For comparison, weak anti-localization was identified[33] in the low-T behavior of Cu_2Se, although with a rather different amplitude and field dependence than what is observed here. Thus though it seems possible that some of the observed response in Cu_2Te is due to such effects, the scaling with resistivity established here points to a classical model based on high mobility threading conduction states as a more reasonable model to explain these observations.

3D Dirac-like electronic states can also lead to a large linear MR, as in the guiding center mechanism recently introduced to account for such cases.[10] However this would be expected to coincide with high overall sample mobility,[9,34–36] as opposed to the situation here. Alternatively, compensation due to multiple carrier pockets[7] might also explain the present results. However it has been shown[27] that hole pockets alone account well for the bulk transport and NMR behavior in $Cu_{2-x}Te$, and observation of linear MR in compositions with different carrier concentrations appears inconsistent with the delicate balance of carriers required for this model. Thus neither of these mechanisms provides a likely explanation for the observed results.

Another consideration would be whether magnetic quantization conditions are reached, such that a quantum MR[11] model is appropriate. Given the effective mass obtained from transport measurements for Cu_2Te and the carrier densities in these samples, we expect[25] that the Fermi energy in the bulk corresponds to several tenths of eV. Even for the case of Dirac-like surface states, with a corresponding Fermi level and assuming the Fermi velocity of graphene, a field of 100 T or more would be required to occupy only the lowest Landau level,[37] with a similarly large field required for 3D states based on the band mass. For the fields applied here we thus expect that many Landau levels will be occupied, a situation far from the quantum limit.

In a discontinuous classical treatment, the linear MR is based on threading currents which percolate[38] through the sample, or at least are well-enough connected to provide the misdirection of currents which has been proposed[39] to underlie this effect. There have been a number of works analyzing this type of transport, including models based on resistor networks[31] as well as in effective medium theories.[38,40] However we are not aware of specific predictions related to the behavior of Fig. 4, which goes smoothly from an inhomogeneous transport-based linear MR to a purely quadratic classic behavior as the temperature and carrier density increases.

A likely source of high mobility threading carriers would be topological surface states, analogous to the silver chalcogenides, and consistent with evidence for inverted band behavior[25] in Cu_2Te. Another possibility might be high mobility carriers such as reported in the layered chalcogenide CuAgSe, attributed to Dirac-like states associated with a bulk band crossing.[41] However NMR measurements also provide a consistent picture of hole pockets with relatively large mass, such as dominate the room-temperature Cu_2Te transport, representing all or most of the Cu sites in the materials,[25,27] so such carriers would be associated with a small-density phase. Since as noted above these carriers should percolate, or at least be well enough connected to provide misdirected transport currents, this points to a thin interface layer rather than isolated inclusions.

Returning to the observed T^2 resistivities, given a thin or 2D interface state in contact with bulk low-mobility carriers, a mechanism for the observed results might be scattering between these two sets of carriers. However with a scattering rate proportional to the density of states, this mechanism would not be expected to produce the observed T^2 dependence even for the 2D case,[42] and the behavior appears to be intrinsic to the high-mobility conducting regions, apparently an effect of enhanced electron-electron interactions. Thus Cu_2Te presents a case where classical linear MR is dominated by strongly-interacting, high mobility threading states, a situation for which there are few experimental examples. For the case of topological surface states as well as for 2D metals in general there has also been considerable interest in understanding the electron-electron interaction behavior.[43,44] In some cases T^2 behavior is predicted analogous with that of ordinary 3D Fermi liquids, through processes that should be strongly dependent on umklapp scattering, and correspondingly on the symmetry and curvature of the Fermi surface.[45,46]

IV. CONCLUSIONS

In conclusion, we observe a large linear magnetoresistance in $Cu_{2-x}Te$ for a range of carrier densities, with the magnitude reaching $\Delta\rho/\rho(0) = 250\%$ at 2 K in a 9 T field, comparable to the effects observed in Ag_2Se and Ag_2Te. Examining the magnitude of the effect vs. the crossover from low-field quadratic to high-field linear behavior, we demonstrated that models based on classical transport best explain the observed results. We also identified a universal scaling between the MR magnitude and the crossover field independent of carrier density. The effects are associated with high-mobility threading states coexisting with the low-mobility bulk carriers, and we discuss mechanisms based on topological surface states or a high-mobility interface phase. There is a crossover to a T^2 resistivity behavior at low temperatures where the large linear MR appears, connected to electron-electron interaction effects within the high mobility threading states, so this system also provides an experimental example of transport behavior in the presence of such strongly interacting states.

ACKNOWLEDGMENTS

This work was supported by the Robert A. Welch Foundation, Grant No. A-1526, and also by the U.S. Department of Energy, with support under the Office of Basic Energy Sciences Award # DE-SC-0008574.

[1] R. Xu, A. Husmann, T. F. Rosenbaum, M.-L. Saboungi, J. E. Enderby, and P. B. Littlewood, Nature **390**, 57 (1997).
[2] A. Husmann, J. B. Betts, G. S. Boebinger, A. Migliori, T. F. Rosenbaum, and M.-L. Saboungi, Nature **417**, 421 (2002).
[3] W. Zhang, R. Yu, W. Feng, Y. Yao, H. Weng, X. Dai, and Z. Fang, Phys. Rev. Lett. **106**, 156808 (2011).
[4] S. Lee, J. In, Y. Yoo, Y. Jo, Y. C. Park, H. jun Kim, H. C. Koo, J. Kim, B. Kim, and K. L. Wang, Nano Lett. **12**, 4194 (2012).
[5] A. Sulaev, P. Ren, B. Xia, Q. H. Lin, T. Yu, C. Qiu, S.-Y. Zhang, M.-Y. Han, Z. P. Li, W. G. Zhu, Q. Wu, Y. P. Feng, L. Shen, S.-Q. Shen, and L. Wang, AIP Advances **3**, 032123 (2013).
[6] J. Kim, A. Hwang, S.-H. Lee, S.-H. Jhi, S. Lee, Y. C. Park, S. in Kim, H.-S. Kim, Y.-J. Doh, J. Kim, and B. Kim, ACS Nano **10**, 3936 (2016).
[7] H. S. Schnyders, Appl. Phys. Lett. **107**, 042103 (2015).
[8] M. Novak, S. Sasaki, K. Segawa, and Y. Ando, Phys. Rev. B **91**, 041203 (2015).
[9] A. Narayanan, M. D. Watson, S. F. Blake, N. Bruyant, L. Drigo, Y. L. Chen, D. Prabhakaran, B. Yan, C. Felser, T. Kong, P. C. Canfield, and A. I. Coldea, Phys. Rev. Lett. **114** (2015).
[10] J. C. W. Song, G. Refael, and P. A. Lee, Phys. Rev. B **92**, 180204 (2015).
[11] A. A. Abrikosov, Phys. Rev. B **58**, 2788 (1998).
[12] S. Hikami, A. I. Larkin, and Y. Nagaoka, Prog. Theor. Phys. **63**, 707 (1980).
[13] M. Veldhorst, M. Snelder, M. Hoek, C. G. Molenaar, D. P. Leusink, A. A. Golubov, H. Hilgenkamp, and A. Brinkman, Phys. Status Solidi (RRL) **7**, 26 (2013).
[14] B. A. Assaf, T. Cardinal, P. Wei, F. Katmis, J. S. Moodera, and D. Heiman, Appl. Phys. Lett. **102**, 012102 (2013).
[15] J. Tian, C. Chang, H. Cao, K. He, X. Ma, Q. Xue, and Y. P. Chen, Sci. Rep. **4**, 4859 (2014).
[16] M. M. Parish and P. B. Littlewood, Nature **426**, 162 (2003).
[17] M. M. Parish and P. B. Littlewood, Phys. Rev. B **72**, 094417 (2005).
[18] C. Herring, J. Appl. Phys. **31**, 1939 (1960).
[19] M. von Kreutzbruck, G. Lembke, B. Mogwitz, C. Korte, and J. Janek, Phys. Rev. B **79**, 035204 (2009).
[20] C. M. Wang and X. L. Lei, Phys. Rev. B **86**, 035442 (2012).
[21] S. Ballikaya, H. Chi, J. R. Salvador, and C. Uher, J. Mater. Chem. A **1**, 12478 (2013).
[22] Y. He, T. Zhang, X. Shi, S.-H. Wei, and L. Chen, NPG Asia Mater. **7**, e210 (2015).
[23] M. C. Nguyen, J.-H. Choi, X. Zhao, C.-Z. Wang, Z. Zhang, and K.-M. Ho, Phys. Rev. Lett. **111**, 165502 (2013).
[24] A. C. Poulose, S. Veeranarayanan, M. S. Mohamed, R. R. Aburto, T. Mitcham, R. R. Bouchard, P. M. Ajayan, Y. Sakamoto, T. Maekawa, and D. S. Kumar, Sci. Rep. **6**, 35961 (2016).
[25] A. A. Sirusi, S. Ballikaya, J.-H. Chen, C. Uher, and J. H. Ross, Jr., J. Phys. Chem. C **120**, 14549 (2016).
[26] Y. Ma, L. Kou, Y. Dai, and T. Heine, Phys. Rev. B **93**, 235451 (2016).
[27] A. A. Sirusi, A. Page, C. Uher, and J. H. Ross, Jr., J. Phys. Chem. Solids **106**, 52 (2017).
[28] H. Nowotny, Z. MetaIlkd. **37**, 40 (1946).
[29] K. Kadowaki and S. Woods, Solid State Communications **58**, 507 (1986).
[30] A. B. Pippard, *Magnetoresistance in metals, Cambridge studies in low temperature physics*: 2 (Cambridge University Press, 1989).
[31] J. Hu, M. M. Parish, and T. F. Rosenbaum, Phys. Rev. B **75**, 214203 (2007).
[32] H. G. Johnson, S. P. Bennett, R. Barua, L. H. Lewis, and D. Heiman, Phys. Rev. B **82**, 085202 (2010).
[33] H. Chi, H. Kim, J. C. Thomas, G. Shi, K. Sun, M. Abeykoon, E. S. Bozin, X. Shi, Q. Li, X. Shi, E. Kioupakis, A. Van der Ven, M. Kaviany, and C. Uher, Phys. Rev. B **89**, 195209 (2014).
[34] T. Liang, Q. Gibson, M. N. Ali, M. Liu, R. J. Cava, and N. P. Ong, Nature Materials **14**, 280 (2014).
[35] Z. Hou, Y. Wang, E. Liu, H. Zhang, W. Wang, and G. Wu, Appl. Phys. Lett. **107**, 202103 (2015).
[36] X. Yang, H. Bai, Z. Wang, Y. Li, Q. Chen, J. Chen, Y. Li, C. Feng, Y. Zheng, and Z. an Xu, Applied Physics Letters **108**, 252401 (2016).

[37] A. H. Castro Neto, F. Guinea, N. M. R. Peres, K. S. Novoselov, and A. K. Geim, Rev. Mod. Phys. **81**, 109 (2009).
[38] D. J. Bergman and D. G. Stroud, Phys. Rev. B **62**, 6603 (2000).
[39] F. Kisslinger, C. Ott, and H. B. Weber, Phys. Rev. B **95**, 024204 (2017).
[40] R. Magier and D. J. Bergman, Phys. Rev. B **74**, 094423 (2006).
[41] S. Ishiwata, Y. Shiomi, J. S. Lee, M. S. Bahramy, T. Suzuki, M. Uchida, R. Arita, Y. Taguchi, and Y. Tokura, Nat. Mater. **12**, 512 (2013).
[42] Y. Xu, Z. Gan, and S.-C. Zhang, Phys. Rev. Lett. **112**, 226801 (2014).
[43] V. E. Sacksteder, K. B. Arnardottir, S. Kettemann, and I. A. Shelykh, Phys. Rev. B **90**, 235148 (2014).
[44] R. Lundgren and J. Maciejko, Phys. Rev. Lett. **115**, 066401 (2015).
[45] H. K. Pal, V. I. Yudson, and D. L. Maslov, Phys. Rev. B **85**, 085439 (2012).
[46] J. M. Buhmann, Phys. Rev. B **88**, 245128 (2013).